Connected-Dense-Connected Subgraphs in Triple Networks

Dhara Shah[1], Yubao Wu[1], Sushil Prasad[1], and Danial Aghajarian[2]

[1] Department of Computer Science, Georgia State University, Atlanta 30303, USA
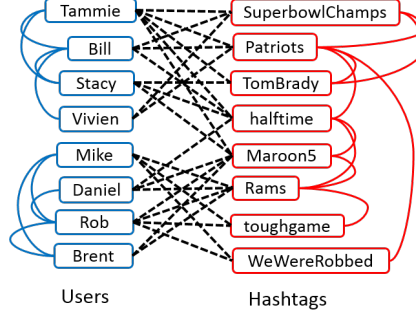`{dshah8, ywu28, sprasad}@gsu.edu`
[2] `daghajarian@cs.gsu.edu`

Abstract. Finding meaningful communities - subnetworks of interest within a large scale network - is a problem with a variety of applications. Most existing work towards community detection focuses on a single network. However, many real-life applications naturally yield what we refer to as Triple Networks. Triple Networks are comprised of two networks, and the network of bipartite connections between their nodes. In this paper, we formulate and investigate the problem of finding Connected-Dense-Connected subgraph (CDC), a subnetwork which has the largest density in the bipartite network and whose sets of end points within each network induce connected subnetworks. These patterns represent communities based on the bipartite association between the networks. To our knowledge, such patterns cannot be detected by existing algorithms for a single network or heterogeneous networks. We show that finding CDC subgraphs is NP-hard and develop novel heuristics to obtain feasible solutions, the fastest of which is O(nlogn+m) with n nodes and m edges. We also study different variations of the CDC subgraphs. We perform experiments on a variety of real and synthetic Triple Networks to evaluate the effectiveness and efficiency of the developed methods. Employing these heuristics, we demonstrate how to identify communities of similar opinions and research interests, and factors influencing communities.

1 Introduction

Community detection is a key primitive with a wide range of applications in real world [7]. Most existing work focuses on finding communities within a single network. In many real-life applications, we can often observe Triple Networks consisting of two networks and a third bipartite network representing the interaction between them. For example, in Twitter, users form a follower network, hashtags form a co-occurrence network, and the user-hashtag interactions form a bipartite network. The user-hashtag interactions represent a user's posts or tweets containing a hashtag. Figure 4 shows a real Twitter Triple Network. The nodes on the left part represent users and those on the right represent hashtags.

Fig. 1. Twitter Triple Network

The edges among the nodes on the left represent a user following other user. The edges among the nodes on the right represent two hashtags appearing in the same tweet. The edges in between represent a user interacting with tweets containing a hashtag. This Triple Network model can ideally represent many real world applications such as taxi pick-up-drop-off networks, Flixster user-movie networks, and author-paper citation networks.

In general, maximizing the density of connections in the Connected-Dense-Connected (CDC) subgraph of a triple network is an unsupervised method for approximating the communities affiliated with the attributes. In the twitter example the density is the number of connections between users and tweets and reflects the degree to which the users are engaged with those tweets. Therefore finding the CDC subgraph is likely to be a useful approach to understanding social and other networks. Given a Triple Network consisting of two graphs $G_a(V_a, E_a)$ and $G_b(V_b, E_b)$ and a bipartite graph $G_c(V_a, V_b, E_c)$, the CDC consists of two subsets of nodes $S \subset V_a$ and $T \subset V_b$ such that the induced subgraphs $G_a[S]$ and $G_b[T]$ are both connected and the density of $G_c[S, T]$ is maximized.

In the Twitter Triple Network in Figure 4, we observe two CDC subgraphs: the one at the top with $S_1 = \{$Tammie, Bill, Stacy, Vivien$\}$ and $T_1 = \{$Patriots, TomBrady, SuperbowlChamps, halftime, Maroon5$\}$, and the one at the bottom with $S_2 = \{$Mike, Daniel, Rob, Brent$\}$ and $T_2 = \{$Rams, toughgame, Maroon5$\}$. In either of the two CDCs, the left and right networks are connected and the middle one is dense. These CDCs are meaningful. The CDC at the top shows that Patriots' fans are praising Tom Brady and are happy to be champions again. The CDC at the bottom shows that LA Rams' fans are disappointed to loose the game.

Our problem is different from finding co-dense subgraphs [11,14] or coherent dense subgraphs [9,13], whose goal is to find the dense subgraphs preserved across multiple networks with the same types of nodes and edges. In our problem, the left and right networks contain different types of nodes and the edges in the three networks represent different meanings. Our problem is also different than the densest connected subgraphs in dual networks [20]. Dual networks consist of one set of nodes and two sets of edges. Triple Networks consist of two sets of nodes and three sets of edges. Triple Networks can degenerate to dual networks

when the two sets of nodes are identical and the bipartite links connect each node to its replica.
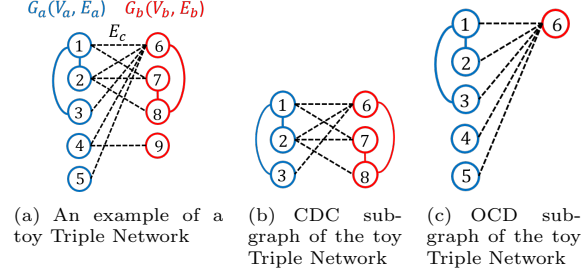
2   Background and related work

The problem of finding a densest subgraph of a graph has been well studied by data mining community. At the core, this problem asks for finding subgraphs with the highest average degree. This problem has been solved in polynomial time using max-flow min-cut approach [8]. Inspired by this approach, the problem of finding densest subgraph in a directed graph has also been solved in polynomial time [12]. The prohibitive cost of these polynomial time algorithms has been addressed with 2-approximation algorithm [6]. However, variations of densest subgraph problems, such as discovery of densest subgraph with k nodes, have been shown to be NP-hard [3]. On the other hand, the problem of finding densest subgraph with pre-selected seed nodes is solvable in polynomial time [15].

The solutions above are designed for homogeneous information network structure where the nodes and edges have just one type. Heterogeneous information networks [18] – the networks with multiple node and edge types – have been a new development in the field of data mining. Heterogeneous network structure provides a model for graph infusion with rich semantics. The Triple Networks introduced in this paper are a type of heterogeneous network with node types V_a and V_b, and edge types E_a, E_b and E_c. Our work can be categorized as unsupervised clustering in heterogeneous network. Parallel to our work, Boden et al. discuss a density based clustering approach of k-partite graphs in heterogeneous information structure [4]. In this work, two types of nodes V_a and V_b are considered. With node type specific hyper-parameters and the bipartite connections E_c, the connections E_a and E_b are inferred. This method of clustering is different from our work where E_a and E_b are part of the network, and the definition of density is hyper-parameter free. Boden et al. detect communities by subspace clustering on nodes' projection to attribute space. In contrast, our work of finding CDC subgraphs cannot be inferred as a subspace clustering technique. Though both works produce iterative refinement algorithms, the former concentrates on improving inference of E_a and E_b iteratively.

The closest network schema to our work is dual networks [20], discovered by Wu et al. A dual network is comprised of two networks having the same set of nodes but different types of edges. These two networks are inferred as physical and conceptual networks. Wu et al. provide 2-approximation algorithms for NP-hard problem of finding subgraphs that are densest in conceptual network, and are connected in physical network. Though the network architecture and subgraph patterns are different, our work is inspired by the pruning methods and variants proposed in this work. To the best of our knowledge there is no comparable algorithm for finding a densest CDC subgraph.

3   Triple network, CDC subgraphs and variants

In this section we define Triple Network, CDC subgraph and its variants. We prove that finding CDC subgraph and variants from a Triple Network is NP-hard.

(a) An example of a toy Triple Network

(b) CDC subgraph of the toy Triple Network

(c) OCD subgraph of the toy Triple Network

Fig. 2. Toy Triple Network and its CDC and OCD subgraphs

Definition 1 (Triple network). *Let $G_a(V_a, E_a)$ and $G_b(V_b, E_b)$ represent graphs of two networks. Let $G_c(V_a, V_b, E_c)$ represent the bipartite graph between G_a and G_b. $G(V_a, V_b, E_a, E_b, E_c)$ is the Triple Network generated by G_a, G_b and G_c.*

We abbreviate a Triple Network as G. An example of Triple Network is illustrated in figure 2(a).

The subgraphs induced by $S_a \subset V_a$ and $S_b \subset V_b$ in networks G_a, G_b and G_c are denoted by $G_a[S_a]$, $G_b[S_b]$ and $G_c[S_a, S_b]$. For brevity, we denote this sub Triple Network, a set of three subgraphs, as $G[S_a, S_b]$.

Definition 2 (Density of a Triple Network). *Given a Triple Network $G[S_a, S_b]$, its density is defined as $\rho(S_a, S_b) = \frac{|E_c(S_a, S_b)|}{\sqrt{|S_a||S_b|}}$, where $|E_c[S_a, S_b]|$ is the number of bipartite edges in subgraph $G_c[S_a, S_b]$, $|S_a|$ is the number of nodes in $G_a[S_a]$ and $|S_b|$ is the number of nodes in $G_b[S_b]$.*

For example, the density of sub Triple Network in figure 2(b) with $S_a = \{1, 2, 3\}$ and $S_b = \{6, 7, 8\}]$ is $\rho(S_a, S_b) = \frac{|E_c(S_a, S_b)|}{\sqrt{|S_a||S_b|}} = \frac{6}{\sqrt{3*3}} = 2$.

By definition of density, only the bipartite edges of a Triple Network contribute to the density. Hence, the density of a Triple Network G is same as the density of its bipartite subgraph G_c.

3.1   Connected-Dense-Connected (CDC) subgraphs

Definition 3 (CDC subgraph). *Given Triple Network $G(V_a, V_b, E_a, E_b, E_c)$, a CDC subgraph is a sub Triple Network $G[S_a, S_b]$ such that*

1. *$G_a[S_a]$ and $G_b[S_b]$ are connected subgraphs, and*

2. *the density $\rho(S_a, S_b)$ is maximized.*

For example, the density of each CDC subgraph in figure 2(b) is 2, higher than density of any other sub Triple Network of the Triple Network 2(a) that is connected in G_a and G_b. A Triple Network can have multiple CDC subgraphs.

Theorem 1. *Finding a CDC subgraph in a Triple Network is NP-Hard.*

Proof. We prove that finding a CDC subgraph is a reduction of set-cover problem. Please refer to [17] for details.

3.2 Variants of CDC subgraph

CDC subgraphs stipulate connectedness of $G_a(S_a)$ and $G_b(S_b)$. Alleviating this connectivity constraint, we define OCD subgraphs for which exactly one of $G_a(S_a)$ or $G_b(S_b)$ is connected.

Definition 4 (OCD subgraph). *Given a Triple Network $G(V_a, V_b, E_a, E_b, E_c)$ a OCD subgraph is a sub Triple Network $G[S_a, S_b]$ such that*

1. *Exactly one of $G_a[S_a]$ or $G_b[S_b]$ is connected, and*
2. *The density $\rho(S_a, S_b)$ is maximized.*

For example, the sub Triple Network $G[\{1, 2, 3, 4, 5\}, \{6\}]$ with the highest density 2.23 in figure 2(c) is an OCD subgraph as $G_a[\{5\}]$ is connected. A Triple Network can have multiple OCD subgraphs.

Adding constraints to CDC and OCD subgraphs We observe that CDC patterns are meaningful around pre-selected nodes in $G_a(S_a)$ or $G_b(S_b)$. We identify these pre-selected nodes as seeds. We introduce CDC and OCD subgraphs with seed constraints, where $G_a(S_a)$ or $G_b(S_b)$ should maintain their connectivity constraints while containing the seeds.

Definition 5. *(CDC_seeds).Given a Triple Network $G(V_a, V_b, E_a, E_b, E_c)$ and sets of seed nodes $V_1 \subset V_a$ and $V_2 \subset V_b$, the CDC_seeds subgraph consists of sets of nodes S_a, S_b such that $V_1 \subset S_a$, $V_2 \subset S_b$, $G_a[S_a]$ and $G_b[S_b]$ are connected and density of $G[S_a, S_b]$ is maximized.*

Definition 6. *(OCD_seed). Given a Triple Network $G(V_a, V_b, E_a, E_b, E_c)$ and a set of node V with $V \subset S$, the OCD_seed consists of sets of nodes such that either $G_a[S]$ or $G_b[S]$ is connected and the density of $G[S, E_c[S]]$ is maximized.*

Finding OCD, CDC_seeds and OCD_seed subgraphs in a Triple Network is NP-hard. Similar set-cover arguments as in Theorem 1 could be used to prove it. Please refer to [17] for details.

4   Heuristic algorithms

Finding CDC subgraphs is NP-hard. Hence in this section, we propose heuristic algorithms for finding feasible solutions. We propose algorithms with following two approaches.

In the first approach, we first obtain the densest bipartite subgraph $G_c[S_a, S_b]$. We then find the connected components of $G_a[S_a]$ and $G_b[S_b]$ using BFS. Thus we obtain connected sub Triple Networks with bipartite edges in $G_c[S_a, S_b]$. We choose the highest density results as feasible CDC subgraphs. Since the time complexity of obtaining densest bipartite subgraph is higher than that of BFS, algorithms in sections 4.1 and 4.2 focus on improving the complexity of finding the densest bipartite subgraphs.

In the second approach, we obtain local CDC subgraphs with given seed nodes from V_a and V_b by adding highest bipartite degree nodes while maintaining the connectedness in G_a and G_b. This Local Search algorithm is presented in section 4.3.

We observe that real-world Triple Networks are sparse in E_c. We also observe that a connected densest subgraph exists for a bipartite graph[16]. Exploiting these virtues, we divide the bipartite graph $G_c[V_a, V_b]$ in to smaller connected bipartite subgraphs and apply the densest subgraph algorithms only for larger subgraphs. This optimization significantly reduces the running-times of our algorithms.

4.1   Maxflow Densest Subgraph (MDS)

MDS algorithm, formalized as Algorithm 1, finds a densest bipartite subgraph of a Triple Network in polynomial time using max-flow min-cut strategies discussed in [12] and [8]. We provide the details of our derivation including proofs, over all approach and examples in [16]. The density difference of any two subgraphs of a bipartite graph $G_c[V_a, V_b]$ is no less than $\frac{1}{|V_a|^2|V_b|^2}$. Hence, the binary search in MDS with step size $\frac{1}{|V_a|^2|V_b|^2}$ halts in $O(|V_a|^{3/2}|V_b|^{3/2})$ iterations. Within each iteration, the min cut is calculated in $O(|V_a|+|V_b|)^2(2(|V_a|+|V_b|)+|E_c|))$. Hence, the complexity of MDS is $O(|V_a|^{4.5}|V_b|^{4.5})$. Adding the cost of BFS for finding connected components in G_a and G_b, the upper-bound still remains unchanged.

Though polynomial time, the prohibitive time complexity of MDS algorithm makes it impracticable to employ for large Triple Networks. By using MDS results on smaller bipartite graphs as a baseline, we develop heuristics in section 4.2.

4.2   Greedy Node Deletions

In this section, we present heuristics to obtain a dense bipartite subgraph with a reduced time complexity.

The first heuristic is to iteratively delete the nodes with the lowest bipartite degree and yield the densest subgraph obtained in the process. This algorithm of

---

Algorithm 1 Maxflow Densest Subgraph (MDS)

Input: Triple Network $G(V_a, V_b, E_a, E_b, E_c)$,with $V_a \neq \phi, V_b \neq \phi$
Output: A densest bi-partite subgraph $G_c[S_a, S_b]$ of G

1: $possible\_ratios = \{\frac{i}{j}| i \in [1, \cdots |V_a|], j \in [1, \cdots |V_b|]\}$

2: $densest\_subgraph = \phi, maximum\_density = \rho(V_a, V_b)$

3: **for** $ratio\ guess\ r \in possible\_ratios$ **do**

4:      $low \leftarrow \rho(V_a, V_b), high \leftarrow \sqrt{|V_a||V_b|}, g = G_c[V_a, V_b]$

5:      **while** $high - low \geq \frac{1}{|V_a|^2|V_b|^2}$ **do**

6:          $mid = \frac{high+low}{2}$

7:          construct a flow graph G' as described in [16] and find the
            minimum s-t cut S, T

8:          $g' = S \setminus \{\text{source node } s\}$

9:          **if** $g' \neq \phi$ **then**

10:              $g \leftarrow g'$

11:              $low = max\{mid, \rho(g)\}$

12:          **else** $high = mid$

13:          **if** $maximum\_density < low$ **then**

14:              $maximum\_density = low$

15:              $densest\_subgraph = g$

Greedy Node Deletion using degrees (GND) is formalized as Algorithm 2, where criterion in line 4 is node degree.

However, degree is not the best measure of a node's impact on density. Figure 2(a) illustrates that GND deletes the nodes $\{3, 4, 5\}$ iteratively. This order of deletions leads to missing the densest bipartite subgraph $[\{1, 2, 3, 4, 5\}, \{6\}]$ in figure 2(c). Instead of accounting for the connections of a node, the percent of the possible connections of that node may serve as a better measure of the node's impact on density. With this intuition, we define rank of a node.

Definition 7 (Rank). *Let $G(V_a, V_b, E_a, E_b, E_c)$ be a Triple Network. For $v_a \in V_a, rank(v_a) = \frac{d(v_a)}{|V_b|}$ and for $v_b \in V_b, rank(v_b) = \frac{d(v_b)}{|V_a|}$.*

Using the lowest rank as the deletion criterion, we modify Algorithm 2 to formulate Greedy Rank Deletion (GRD) algorithm where the criterion of deletion in line 4 is rank.

GND and GRD delete nodes sequentially. To expedite this process, we delete all the nodes satisfying the deletion criterion in bulk in each iteration instead. This idea is formulated as fast Rank Deletion (FRD) Algorithm in 3. These bulk deletions do not lower the time complexity upper-bound, but the number of iterations decreases exponentially. The deletion criterion of FRD could be tuned by choosing different ϵ values from $(-1, 1)$ with ϵ values from lower to higher resulting in less to more deletions per iteration.

By maintaining two {degree:node} Fibonacci heaps and an index on the nodes, the time complexity of these greedy deletion algorithms is $O((V_a+V_b)log(V_a+$

$V_b) + E_c$). Adding the cost of BFS for connected components in G_a and G_b, the total time complexity for obtaining CDC subgraphs is $O((V_a + V_b)log(V_a + V_b) + E_c + E_a + E_b)$.

Algorithm 2 Greedy Node Deletions	**Algorithm 3** Fast Rank Deletion (FRD)
Input: Triple Network $G(V_a, V_b, E_a, E_b, E_c)$,with $V_a \neq \phi, V_b \neq \phi,$ *criterion* to delete nodes **Output:** A densest subgraph $G_c[S_a, S_b]$ of G	**Input:** Triple Network $G(V_a, V_b, E_a, E_b, E_c)$,with $V_a \neq \phi, V_b \neq \phi,$ value of $\epsilon \in (-1, 1)$ **Output:** A densest bi-partite subgraph $G_c[S_a, S_b]$ of G

Algorithm 2 Greedy Node Deletions

1: $S_a = V_a, S_b = V_b$
2: $maximim\_density = \rho(V_a, V_b)$
3: **while** $V_a \neq \phi$ *and* $V_b \neq \phi$ **do**
4:    v = node with minimum *criterion* in $V_a \cup V_b$
5:    $V_a = V_a \setminus \{v\}, V_b = V_b \setminus \{v\}$
6:    **if** $maximum\_density < \rho(V_a, V_b)$ **then**
7:      $S_a = V_a, S_b = V_b,$
8:      $E_c = E_c[V_a, V_b]$
9: **return** $G_c[S_a, S_b]$

Algorithm 3 Fast Rank Deletion (FRD)

1: $S_a = V_a, S_b = V_b,$
2: $maximim\_density = \rho(V_a, V_b)$
3: **while** $V_a \neq \phi$ *and* $V_b \neq \phi$ **do**
4:    $\bar{r}$ = average node rank in G
5:    $\bar{V} = \{v \in V_a \cup V_b \,|\, rank(v) < (1 + \epsilon)\bar{r}\}$
6:    $V_a = V_a \setminus \bar{V}, V_b = V_b \setminus \bar{V}$
7:    **if** $maximum\_density < \rho(V_a, V_b)$ **then**
8:      $S_a = V_a, S_b = V_b,$
9:      $E_c = E_c[V_a, V_b]$
10: **return** $G_c[S_a, S_b]$

Algorithm 4 Local Search (LS)

Input: $G(V_a, V_b, E_a, E_b, E_c)$,with $V_a \neq \phi, V_b \neq \phi$
     $seedS_a$ = Set of seeds in V_a
     $seedS_b$ = Set of seeds in V_b
Output: A sub Triple Network $G[S_a, S_b]$ of G

1: S_a = Spanning tree of $seedS_a$ in G_a
2: S_b = Spanning tree of $seedS_b$ in G_b
3: $\delta(S_a) = \{v \notin S_a | \ S_a$ contains v's neighbor in $G_a\}$,Boundary of S_a in G_a
4: $\delta(S_b) = \{v \notin S_b | \ S_b$ contains v's neighbor in $G_b\}$, Boundary of S_b in G_b
5: $nbhd$, the adjacency list of V_a in G_a and V_b in G_b
6: $max\_density = \rho(G[S_a, S_b])$
7: **do**
8:    v = node in $\delta(S_a) \cup \delta(S_b)$ with the highest bi-partite connections to $S_a \cup S_b$
9:    $S_a = S_a \cup v$ if $v \in V_a$, $S_b = S_b \cup v$ if $v \in V_b$
10:    $\delta(S_a) \cup \delta(S_b) = \delta(S_a) \cup \delta(S_b) \cup nbhd(v) \setminus \{v\}$
11:    $max\_density = max(max\_density, \rho(G[S_a, S_b]))$
12: **while** $\rho(G_c[S_a, S_b]) \geq max\_density$ *and* $\delta(S_a) \cup \delta(S_b) \neq \phi$;
13: **return** $G[S_a, S_b]$

4.3   Local Search

In this section, we introduce Local Search (LS), a bottom-up approach for obtaining CDC subgraphs around seeds – pre-selected nodes. Let S_a and S_b be the spanning trees of desired seeds in V_a and V_b. LS, outlined as Algorithm 4, iteratively includes previously un-included boundary node of $S_a \cup S_b$ with the maximum adjacency value to the set of included nodes. LS hence finds CDC subgraph by adding nodes that increase the density while maintaining connectedness of S_a and S_b.

As illustrated in experiments, LS yields local patterns with good semantic value. In practice, the search stops in a few iterations and hence LS is emperially the fastest algorithm yet.

4.4   Algorithms for variants

We obtain OCD subgraphs as bi-products of mining CDC subgraphs. For MDS and Greedy Node Deletions, the resultant sub Triple Networks maintaining exactly one connectedness with the highest density are yielded as OCD subgraphs. We instantiate LS algorithm with either S_a or S_b to be empty and obtain CDC_seeds and OCD_seed subgraphs.

5   Experiment results

In this section, we evaluate the effectiveness and efficiency of the proposed methods through comprehensive experiments on real and synthetic datasets. We demonstrate the effectiveness of CDC and OCD subgraphs by illustrating novelty of the information obtained from these subgraphs on real Triple Networks. We demonstrate the efficiency of our algorithms by measuring the running times of the algorithms and the density of the resultant CDC subgraphs. The programming language employed is Python 2.7 and the experiments were conducted on Intel Core i7 3.6Gz CPU with 32G memory.

5.1   Real Triple Networks

We employ Triple Networks constructed from Twitter, NYC taxi data, Flixter and ArnetMiner coauthor datasets. Table 1 describes the statistics of these real Triple Networks.

NYC Taxi data New York City (NYC) yellow cab taxi data is a dataset [1] where each taxi trip's pick-up and drop-off point is a geographic location in decimal degrees. We consider the trips from June 2016 to construct a Triple Network. The geographic location accuracy of this dataset is thresholded up to 5 decimal points, preserving granularity to different door-entrances. Hence G_a and G_b are the networks of pick-up and drop-off points. In these networks, edges connect the points within 50 meters of haversine distance. The taxi trips are represented as E_c.

Twitter network Twitter is a social media for micro-blogging where users can follow each other for updates. To extract meaningful user-follower relationships, we choose popular news networks, namely CNN, Huffington Post and Fox News, and randomly extract a few thousand of their intersecting followers. We iteratively grow this network by including followers of existing nodes using Twitter's REST API. At each iteration, we threshold users by number of recent tweets and number of followers. Thus, we construct a 5-hop users-followers network G_a, where two users are connected if one follows the other. We collect different hashtags from these users' tweets with E_c as users posting hashtags. We consider two hashtags connected if they appear in the same tweet, and thus construct hashtag co-occurance network as G_b.

ArnetMiner Coauthor data ArnetMiner Coauthor dataset [19] is comprised of two types of networks: authors and their co-author relationships as G_a, and their research interests as G_b, with E_c as relations of authors to their research interests. We consider two research interests linked if they co-occur in an other's list of research interests.

Flixter data Flixter [10] is a social network of users and their movie ratings. We consider the users social network as G_a, the users' rankings of movies as E_c, and movies as V_b. With no sufficient information, we consider $|E_b| = 0$.

Table 1. Real triple-networks on NY Taxi data (TX), Twitter (TW), ArnetMiner (AM), and Flixter (FX) data

Data	$|V_a|$	$|E_a|$	$|V_b|$	$|E_b|$	$|E_c|$
TX	733896	31513503	794085	13465065	2066569
TW	61726	7008491	3679824	2896925	48269139
AM	1712433	4258946	3901018	953490	12589981
FX	786936	7058819	48794	0	8196077

Table 2. Synthetic Random and R-MAT networks

$|V_a|$	$|E_a|$	$|V_b|$	$|E_b|$	$|E_c|$
2^{19}	5×10^6	2^{19}	5×10^6	10^7
2^{20}	10^7	2^{20}	10^7	2×10^7
2^{21}	2×10^7	2^{21}	2×10^7	4×10^7
2^{22}	4×10^7	2^{22}	4×10^7	8×10^7

5.2   Synthetic Triple Networks

We generated random networks with synthetic G_a, G_b and G_c having random edges in order to evaluate efficiency of our algorithms. To approximate real world Triple Networks, we also generated R-MAT networks with G_a and G_b having R-MAT edges [5,2] and G_c having random edges. We generated four different configurations for random and R-MAT networks (see Table 2). To the best of our knowledge, there are no algorithms to obtain CDC subgraphs. However, the MDS algorithm provides the densest bipartite subgraph, and hence is an upper-bound to the density of CDC. The high time complexity of MDS algorithm limits its applicability with real problems and thus we used synthetic benchmarks.

5.3   Effectiveness Evaluation on Real Networks

We illustrate the effectiveness of CDC subgraphs and variants by emphasizing the knowledge gain from these patterns obtained from real networks. These figures demonstrate that CDC subgraphs and variants are communities detected by the

$|V_a| = |V_b|$	$|E_a| = |E_b|$	$|E_c|$	Random networks: MDS/GRD bipartite	RMAT networks: MDS/GRD bipartite
2^{15}	3.125×10^5	6.25×10^5	0.9897	1.1970
2^{16}	6.25×10^5	1.25×10^6	0.9901	1.1898
2^{17}	1.25×10^6	2.5×10^6	0.9865	1.2101
2^{18}	2.5×10^6	5×10^6	1.0010	1.1985
2^{19}	5×10^6	10^7	0.9753	1.2021

Table 3. Caption

(a) CDC subgraph yielding directional flow of human migration in 1 hour period

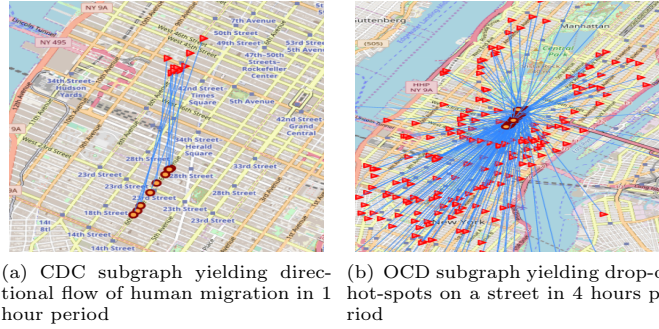(b) OCD subgraph yielding drop-off hot-spots on a street in 4 hours period

Fig. 3. CDC and OCD subgraphs from NY Taxi data. Triangles and circles represent pick-up and drop-off points respectively

(a) CDC subgraph representing Patriots' fans
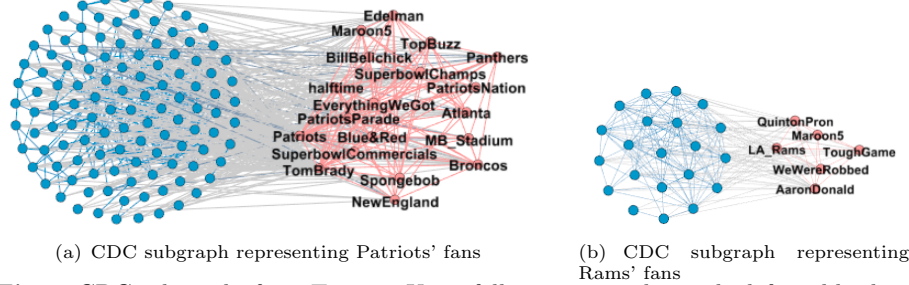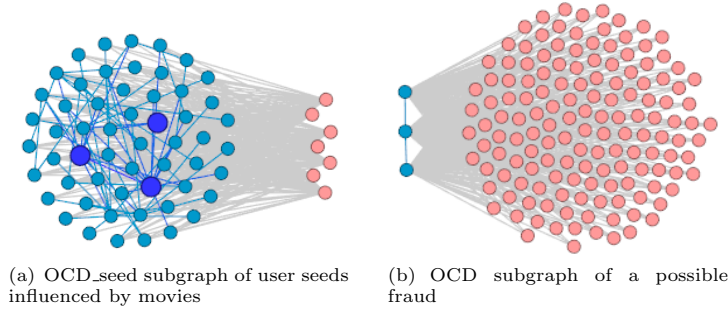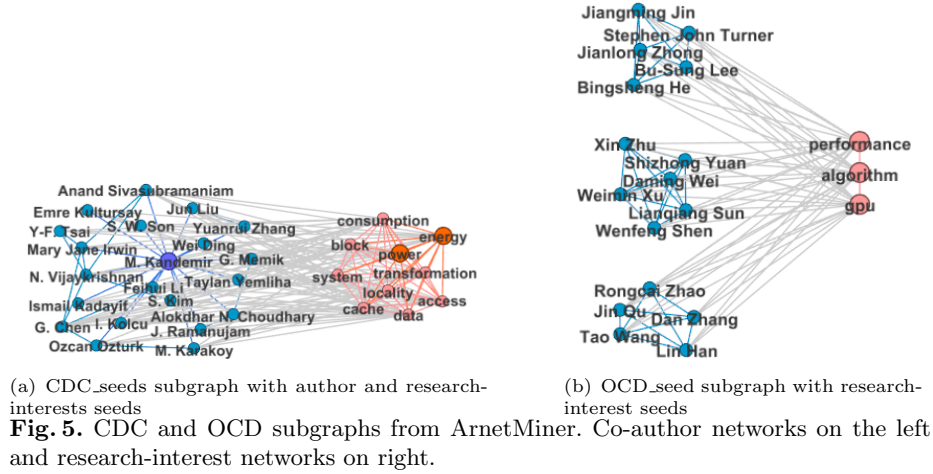
(b) CDC subgraph representing Rams' fans

Fig. 4. CDC subgraphs from Twitter. Users-followers networks on the left and hashtag networks on the right.

strong associations to their attributes. These subgraphs identify similar opinions, research interests and factors influencing communities. They are also effective tools for hot-spot detection and fraud detection.

NYC Taxi data Figure 3 illustrates CDC and OCD subgraphs with pick-up and drop-off points as triangles and circles respectively.

Figure 3(a) illustrates the CDC subgraph with pick-up locations on 6th Avenue between 18th and 27th street populated with food and shopping destinations, and drop-of locations on 8th Avenue. This CDC subgraph is generated by observing the 6:00-7:00 pm traffic on June 4, 2016. The drop-off points are clustered near 42nd street Port Authority bus terminals of city transit. This CDC subgraph gives a directional flow of human migration in a short distance during a specific time-frame. Figure 3(b) illustrates OCD subgraph with pick-up seeds

(a) CDC_seeds subgraph with author and research-
interests seeds

(b) OCD_seed subgraph with research-
interest seeds

Fig. 5. CDC and OCD subgraphs from ArnetMiner. Co-author networks on the left
and research-interest networks on right.

(a) OCD_seed subgraph of user seeds
influenced by movies

(b) OCD subgraph of a possible
fraud

Fig. 6. OCD subgraphs from Flixter. User networks on the left and movie networks
on the right.

near 5th Avenue and Central Park South. This subgraph is generated by observ-
ing 4:00-8:00 pm traffic on June 1, 2016. The pick-up points are scattered along
Manhattan and the drop-off points are clustered around Pennsylvania Station,
a public transit hub. Thus, OCD subgraphs could be equivalents to hot-spot
detection.

Twitter Network Figure 4 represents CDC subgraphs obtained from Twitter
Network. Left and right subgraphs represent users-followers and hashtag net-
works. We remove usernames to protect user privacy. These figures represent
twitter users and their opinions about SuperBowl contenders, Patriots and LA
Rams. Hence, CDC subgraphs can identify communities with contrasting opin-
ions.

ArnetMiner coauthor data Figure 5 depicts CDC_seeds and OCD_seed sub-
graphs from ArnetMiner Triple Network. Left and right subgraphs represent
author-coauthor and research-interest networks.

Figure 5(a) is a CDC_seeds subgraph with randomly chosen author seed
{M.Kandimir} and interest seeds {power,energy}. This pattern yields author
seed's associates working on related research topics of interest seeds. Figure 5(b)

is OCD_seed subgraph with interest seeds chosen as {algorithm, gpu, performance}. This patterns yields 16 authors and their respective co-author networks with publications related to interests seeds. Thus, even with the given seeds, the CDC and OCD subgraphs are different from supervised community detection.
Flixter data Figure 6 depicts OCD subgraphs illustrating influence of movies on users. Left and right subgraphs represent the users' social networks and the movies networks, The users networks are connected.

Figure 6(a) is an OCD_seed subgraph with users seeds, chosen at random. The right network represents movies with 5 star rankings by the users on the left. This pattern hence finds the movies influencing the friend-circle of the seed users. An OCD subgraph in figure 6(b) depicts a suspicious ranking activity, where the 3 users on the left give a 5 star ranking to 144 movies on the right. CDC and OCD subgraphs hence illustrate the power of potential fraud detection.
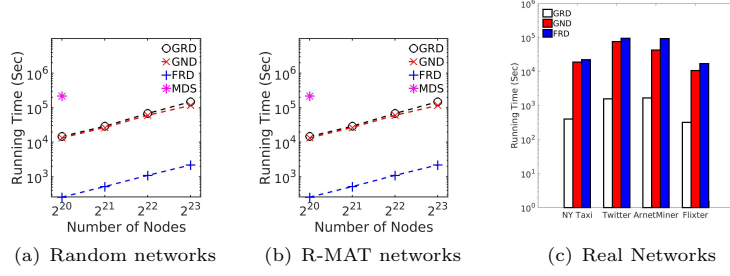
5.4   Efficiency evaluation

We evaluate the efficiency of our heuristic algorithms by their running-time and the quality of the resulting CDC subgraphs from real and synthetic networks.

Greedy node deletions The running-times of MDS, GND, GRD, FRD algorithms on real, random and R-MAT networks are depicted in Figure 7. The x axis represents the number of nodes in $V_a \cup V_b$ and the y axis represents log scale of seconds. Each point represents running-time of the algorithm for given network. The running-time of MDS algorithm for larger networks is more than 24 hours, when we halted the algorithm computations. Running-times increase with network size, but vary a little for random and R-MAT graphs of the same size. FRD with $\epsilon = 0$ is the fastest algorithm.

We discover that GRD yields the densest bipartite subgraph among all algorithms. The densities of CDC subgraphs obtained by GND, GRD and FRD from random and R-MAT networks are presented in table 4 and 5. For each graph, DBP represents the density of the densest bipartite graph obtained by GRD, without being connected in G_a or G_b. The ratio, DBP/CDC densitiy, varies a little with the network size. This trend is observed across all network types and algorithms. GRD produces the best and FRD with $\epsilon = 0$ produces the least accurate results.
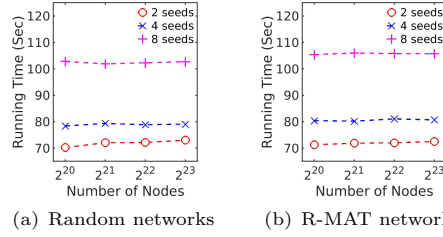
Local Search (LS) Given the seeds of V_a and V_b, LS produces meaningful, locally dense CDC patterns. We evaluate the efficiency of LS algorithm by measuring its running-times with 2, 4 and 8 seeds. Figure 8 presents the running-times of LS. The x axis represents the number of nodes in $V_a \cup V_b$ and the y axis represents running-times in seconds. Each point represents running-time of FRD for given network and seed configuration. The seeds are chosen randomly in the same connected components. The boundaries $\delta(S_a)$ and $\delta(S_b)$ grow larger with increase in the number of seeds. Hence the running-time of LS increases with the number of seeds. We observe similar trends from real networks. In synthetic

(a) Random networks   (b) R-MAT networks   (c) Real Networks

Fig. 7. Running-times for MDS, GND, GRD and FRD

Table 4. CDC subgraph densities from random networks

	2^{20}	2^{21}	2^{22}	2^{23}
DBP	19.083	19.095	19.094	19.086
GND	18.713	18.705	18.691	18.720
GRD	18.901	18.836	18.837	18.698
FRD	7.401	7.389	7.402	7.401

Table 5. CDC subgraph densities from R-MAT networks

	2^{20}	2^{21}	2^{22}	2^{23}
DBP	19.071	19.065	19.073	19.072
GND	17.028	16.761	17.019	16.627
GRD	17.201	17.002	17.046	16.689
FRD	6.612	6.610	6.509	6.501

(a) Random networks   (b) R-MAT networks

Fig. 8. LS running-times with 2,4 and 8 seeds

networks, for a given number of seeds, LS running-times vary a little across different network sizes. This is because LS halts when the density of the current CDC subgraph starts decreasing, which depends only on the local topologies of G_a and G_b.

Fast Rank Deletion (FRD) The purpose of FRD is to obtain feasible CDC subgraphs faster. This is achieved by deleting all the nodes with degree less than $(1 + \epsilon) * average\ degree$ at each pass. However, lower ϵ values result in fewer deletions per pass, defying the purpose of FRD. Higher ϵ values result in more deletions per pass, lowering the densities of the resulting CDC subgraphs. Hence the meaningful results are obtained with ϵ values in the range of interval $[-0.4, 0.4]$.

Figures 9(a) and 9(b) represent the running-times of FRD. The x axis represents different ϵ values and the y axis represents running-times in log scale of seconds. Each point represents running-time of FRD for given network and ϵ configurations. Increase in ϵ value causes higher amount of deletion per pass,

(a) Random networks(b) R-MAT networks(c) Random networks(d) R-MAT networks

Fig. 9. FRD evaluations for $\epsilon \in [-0.4, 0.4]$

resulting in fewer passes. Hence, the running-times decrease with the increase of ϵ.

Figures 9(c) and 9(d) represent the density change of resultant CDC subgraphs for given ϵ value, with respect to $\epsilon = 0$. The x axis represents different ϵ values, and the y axis represents the ratio, Density of CDC for $\epsilon = 0$/Density of CDC with given ϵ. Each point represents this density ratio obtained by FRD, for given network and ϵ configurations. Higher ϵ values result in more deletions per pass, lowering the densities of the resulting CDC subgraphs. Hence, the density ratio increases as the ϵ value decreases. We observe similar trends from real networks. The densities of resultant CDC subgraphs obtained by FRD depend on network topologies. Hence, for the same type of synthetic networks with the same ϵ value, the variance in the density ratio is low.

6   Conclusion

In this paper, we introduce Triple Network, its CDC subgraph problem and its variants. We provide heuristics to find feasible solutions to these patterns, otherwise NP-Hard to find. We conclude that CDC subgraphs yield communities with similar charasteristics by illustrating the information gain of these patterns in NYC taxi, Twitter, ArnetMiner, and Flixter networks. We demonstrate the efficiency of our algorithms on large real and synthetic networks by observing running-time and density trends in real and synthetic networks.

References

1. NYC taxi & limousine commission - trip record data, `https://www1.nyc.gov/site/tlc/about/tlc-trip-record-data.page`
2. Bader, D.A., Madduri, K.: Gtgraph: A synthetic graph generator suite. Atlanta, GA, February (2006)
3. Bhaskara, A., Charikar, M., Chlamtac, E., Feige, U., Vijayaraghavan, A.: Detecting high log-densities: an o (n 1/4) approximation for densest k-subgraph. In: Proceedings of the forty-second ACM symposium on Theory of computing. pp. 201–210. ACM (2010)
4. Boden, B., Ester, M., Seidl, T.: Density-based subspace clustering in heterogeneous networks. In: Joint European Conference on Machine Learning and Knowledge Discovery in Databases. pp. 149–164. Springer (2014)

5. Chakrabarti, D., Zhan, Y., Faloutsos, C.: R-mat: A recursive model for graph mining. In: Proceedings of the 2004 SIAM International Conference on Data Mining. pp. 442–446. SIAM (2004)
6. Charikar, M.: Greedy approximation algorithms for finding dense components in a graph. In: International Workshop on Approximation Algorithms for Combinatorial Optimization. pp. 84–95. Springer (2000)
7. Fortunato, S.: Community detection in graphs. Physics reports **486**(3-5), 75–174 (2010)
8. Goldberg, A.V.: Finding a maximum density subgraph. University of California Berkeley, CA (1984)
9. Hu, H., Yan, X., Huang, Y., Han, J., Zhou, X.J.: Mining coherent dense subgraphs across massive biological networks for functional discovery. Bioinformatics **21**(suppl_1), i213–i221 (2005)
10. Jamali, M., Ester, M.: A matrix factorization technique with trust propagation for recommendation in social networks. In: Proceedings of the fourth ACM conference on Recommender systems. pp. 135–142. ACM (2010)
11. Kelley, R., Ideker, T.: Systematic interpretation of genetic interactions using protein networks. Nature biotechnology **23**(5), 561 (2005)
12. Khuller, S., Saha, B.: On finding dense subgraphs. In: International Colloquium on Automata, Languages, and Programming. pp. 597–608. Springer (2009)
13. Li, W., Hu, H., Huang, Y., Li, H., Mehan, M.R., Nunez-Iglesias, J., Xu, M., Yan, X., Zhou, X.J.: Pattern mining across many massive biological networks. In: Functional coherence of molecular networks in bioinformatics, pp. 137–170. Springer (2012)
14. Pei, J., Jiang, D., Zhang, A.: On mining cross-graph quasi-cliques. In: Proceedings of the eleventh ACM SIGKDD international conference on Knowledge discovery in data mining. pp. 228–238. ACM (2005)
15. Saha, B., Hoch, A., Khuller, S., Raschid, L., Zhang, X.N.: Dense subgraphs with restrictions and applications to gene annotation graphs. In: Annual International Conference on Research in Computational Molecular Biology. pp. 456–472. Springer (2010)
16. Shah, D., Prasad, S., Aghajarian, D.: Finding densest subgraph in a bi-partite graph. Department of Computer Science, Georgia State University, Atlanta, GA (2019), `https://scholarworks.gsu.edu/computer_science_technicalreports/1/`
17. Shah, D., Prasad, S., Wu, Y.: Finding Connected-Dense-Connected Subgraphs and variants is NP-Hard. Department of Computer Science, Georgia State University, Atlanta, GA (2019), `https://scholarworks.gsu.edu/computer_science_technicalreports/2/`
18. Sun, Y., Yu, Y., Han, J.: Ranking-based clustering of heterogeneous information networks with star network schema. In: Proceedings of the 15th ACM SIGKDD international conference on Knowledge discovery and data mining. pp. 797–806. ACM (2009)
19. Tang, J., Zhang, J., Yao, L., Li, J., Zhang, L., Su, Z.: Arnetminer: extraction and mining of academic social networks. In: Proceedings of the 14th ACM SIGKDD international conference on Knowledge discovery and data mining. pp. 990–998. ACM (2008)
20. Wu, Y., Jin, R., Zhu, X., Zhang, X.: Finding dense and connected subgraphs in dual networks. In: Data Engineering (ICDE), 2015 IEEE 31st International Conference on. pp. 915–926. IEEE (2015)